Cerebral Cortex Advance Access published August 14, 2012

Cerebral Cortex
doi:10.1093/cercor/bhs240

Activation-Dependent Subcellular Distribution Patterns of CB1 Cannabinoid Receptors in the Rat Forebrain

Karine Thibault[1,†], Damien Carrel[1,†], Damien Bonnard[1], Katalin Gallatz[2], Anne Simon[1], Marc Biard[1], Sophie Pezet[1], Miklos Palkovits[2] and Zsolt Lenkei[1]

[1]Laboratoire de Neurobiologie, ESPCI-CNRS UMR 7637, ESPCI-ParisTech, Paris 75005, France and [2]Laboratory of Neuromorphology, Semmelweis University and Hungarian Academy of Sciences, 1094 Budapest, Hungary

[†]K.T. and D.C. contributed equally to this work
Address correspondence to Zsolt Lenkei, Laboratoire de Neurobiologie, ESPCI-CNRS UMR 7637, ESPCI-ParisTech, 10 rue Vauquelin, Paris 75005, France. Email: zsolt.lenkei@espci.fr

Chronic cannabinoid exposure results in tolerance due to region-specific desensitization and down-regulation of CB1 cannabinoid receptors (CB1Rs). For most G-protein-coupled receptors, internalization closely follows rapid desensitization as an important component of long-term down-regulation. However, in vivo patterns of CB1R internalization are not known. Here we investigate the subcellular redistribution of CB1Rs in the rat forebrain following activation by agonist CP55 940 or inhibition by antagonist/inverse agonist AM251. At steady state, CB1Rs are mainly localized to the cell membrane of preterminal axon shafts and, to a lesser degree, to synaptic terminals. A high proportion of CB1Rs is also localized to somatodendritic endosomes. Inhibition of basal activation by acute AM251 administration decreases the number of cell bodies containing CB1R-immunoreactive endosomes, suggesting that CB1Rs are permanently activated and internalized at steady state. On the contrary, acute agonist treatment induces rapid and important increase of endosomal CB1R immunolabeling, likely due to internalization and retrograde transport of axonal CB1Rs. Repeated agonist treatment is necessary to significantly reduce initially high levels of axonal CB1R labeling, in addition to increasing somatodendritic endosomal CB1R labeling in cholecystokinin-positive interneurons. This redistribution displays important region-specific differences; it is most pronounced in the neocortex and hippocampus and absent in basal ganglia.

Keywords: axon, basal ganglia, endocytosis, redistribution, tolerance

Introduction

Repeated administration of cannabinoids results in attenuated responsiveness, or tolerance, essentially through desensitization and downregulation of type-1 cannabinoid receptors (CB1Rs) (Hoffman et al. 2003, 2007; Sim-Selley, 2003;Howlett et al., 2004; Martin et al., 2004; Gonzalez et al. 2005). Generally, G-protein-coupled receptors (GPCRs) display 3 overlapping processes in response to agonists over a time scale ranging from seconds to days: rapid desensitization (seconds to minutes), internalization (minutes to hours) and down-regulation (hours to days) (Ferguson 2001; Tsao et al. 2001). The highly conserved mechanism of rapid desensitization involves receptor phosphorylation followed by interaction with cytoplasmic arrestins, which leads to functional uncoupling from G-proteins. Next, phosphorylated and arrestin-bound receptors are internalized from the cell membrane to endosomes, without any notable change in the total number of receptors. Subsequently, internalized receptors are either dephosphorylated and recycled to the cell membrane (resensitization) or degraded in lysosomes. Finally, prolonged agonist exposure leads to a decrease in receptor protein levels, known as down-regulation, caused either by receptor degradation, decrease in receptor synthesis or both, ultimately resulting in fewer available ligand-binding sites.

CB1R desensitization and long-term down-regulation vary in magnitude and time-course across different brain regions, displaying the highest degree of adaptation in the neocortex and hippocampus and the lowest in basal ganglia. These differences are well correlated with differences in the rate of tolerance development associated with each brain region (Sim-Selley 2003; Martin et al. 2004; Gonzalez et al. 2005). While it is likely that CB1R internalization, which is readily detectable in cell culture models (Hsieh et al. 1999; Jin et al. 1999; Coutts et al. 2001; Leterrier et al. 2004, 2006), closely follows rapid desensitization and is an important component of long-term down-regulation, in vivo internalization pattern of CB1R remains unknown. Moreover, because desensitization and down-regulation are greater in magnitude and more regionally widespread among CB1Rs than other GPCRs, such as μ opioid or 5-HT_{1A} receptors (Sim et al. 1996; Sim-Selley et al. 2000), and because of the high level of CB1R expression and the lipophilic nature of endocannabinoids, recent studies have suggested the possibility of distinct adaptive mechanisms (Martin et al. 2004; Childers 2006).

In order to understand the interplay between CB1R activity and subcellular distribution, here we have investigated CB1R localization in several rat forebrain areas following systemic treatment with the agonist CP55 940 or the antagonist/inverse agonist AM251. Our results demonstrate distinctive regional patterns of internalization and somatodendritic accumulation of CB1Rs following agonist treatment in several forebrain areas; conversely, treatment with AM251 results in a significant reduction in the number of cell bodies containing CB1R-immunoreactive endosomes, suggesting that CB1Rs are basally active and internalized at steady state.

Materials and Methods

Chemicals

CP55 940 and AM251 were obtained from Tocris (Bristol, UK). They were dissolved at a final concentration of 1.32 mg/mL in vehicle solution, made of 843 μL NaCl 0.9%, 132 μL absolute ethanol, and 25 μL Tween 80 per mL.

Animal Treatments

Animal experiments were carried out in accordance with the European Community Council Directive of 24 November 1986 (86/609/EEC) regarding the care and use of animals for experimental

procedures. Adult male Sprague–Dawley rats weighing 280–330 g were housed in a 12–12-h light–dark cycle room at 22°C and were provided with free access to food and water. Animals received early-morning intraperitoneal injections of 0.75 mg/kg CP55 940 and/or 3 mg/kg AM251 or 2.73 mL/kg vehicle (VE).

Experimental groups of rats received either CP55 940, AM251, or vehicle and were perfused either 2 h later (CP 2 h, AM 2 h, and VE 2 h groups, $n = 4$) or 16 h later (CP 16 h, AM 16 h, and VE 16 h groups, $n = 3$). Another 2 groups of rats ($n = 3$) received either AM251 or vehicle and were perfused after 4 h (AM 4 h and VE 4 h groups). To test the effects of repeated agonist treatment, 3 experiments were performed. For immunoperoxidase experiments, 2 groups of rats received either CP55 940 ($n = 6$) or vehicle ($n = 3$) daily for 3 days and were perfused 2 h after the last injection, yielding the CP $3x + 2$ h and VE $3x + 2$ h groups. For immunofluorescence experiments, 3 groups of rats received either CP55 940 (CP $3x + 2$ h, $n = 3$), CP55 940 + AM251 (CP + AM $3x + 2$ h, $n = 3$), or vehicle (VE $3x + 2$ h, $n = 4$) daily for 3 days and were perfused 2 h after the last injection. Finally, for the behavioral tests and western blot quantification, the CP $3x + 2$ h ($n = 9$) and VE $3x + 2$ h ($n = 6$) treatments were repeated, and each animal was tested with hot plate and bar tests once before the first treatment to establish the baseline, then 30 min after each treatment. Two hours after the last test on the third day, 3 randomly chosen animals from each group were decapitated and processed for a western blot assay of CB1R protein levels. Finally, we perfused several animals with glutaraldehyde-containing fixative for each acute treatment groups (2- and 4-h groups); for qualitative ultrastuctural analysis, we used light microscopy to select animals which were representative for the treatment group, that is, showing the same overall distribution of CB1Rs as the majority of animals in the corresponding treatment group.

Bar Test

The bar apparatus used to evaluate catalepsy consisted of a 280-mm horizontal bolt (10 mm in diameter) attached to a frame by eye bolts. Bar height was 130 mm. The parameter measured was the total amount of time (in seconds) during which the rat maintained both forepaws in contact with the bar after being placed on the apparatus. Cut-off time was 300 s. This value was expressed as a percentage of maximum time (cut-off) on the bar.

Hot Plate Test

Animals were placed on a hot plate (heated metallic surface at 52°C). The time latency in seconds for the rat to shake or to lick hind paws was recorded using a cut-off time of 15 s (designated to prevent injury to the animal). The antinociceptive effect was expressed as follows: % time on hot plate = 100 × (time latency)/15 s (cut-off time).

Perfusion

Animals were anesthetized with a ketamine/xylazine-hydrochloride combination. For standard immunohistochemistry, animals were fixed by transcardial perfusion of 300 mL of Zamboni's fixative (4% paraformaldehyde and 15% saturated picric acid in 0.1 M phosphate buffer [PB], which is 11.36 g/L Na_2HPO_4, 2.40 g/L NaH_2PO_4 in bidistillated water, pH 7.2), then brains were postfixed in the same solution overnight at 4°C and cryoprotected in sucrose (20% D-saccharose in 0.1 M PB) for 24 h. For the immunoperoxidase experiments, brain regions including the hippocampus were sliced in a freezing microtome to obtain 50-μm–thick coronal sections. For the immunofluorescence experiments, 20-μm–thick coronal brain sections were serially cut using a cryostat. For electron microscopy, rats were perfused with 300 mL Zamboni's fixative containing 0.83% glutaraldehyde (Sigma-Aldrich Kft), then brains were postfixed overnight in Zamboni's fixative at 4°C. Coronal sections (50 μm thick) of brains were made using a vibratome.

Immunochemistry

The anti-CB1R C-terminal (C-Ter) antibody was produced by Eurogentec. As previously described, the C-Ter antibody was produced by injection of a peptide corresponding to the last 14 C-terminal residues (positions 459–473) of the rat CB1R in rabbits followed by affinity purification of sera against the 459–473 peptide (Leterrier et al. 2004). The specificity of the purified C-Ter antibody (Leterrier et al. 2004, 2006) was assessed by comparing immunolabeling on brain sections of wild type and $CB1^{-/-}$ mice (gift from C Ledent); the former demonstrated an immunolabeling comparable to control rat brain sections, and the latter were devoid of any staining (Supplementary Fig. 1*B*). We also verified immunostaining on brain sections of control rats by omitting antibody and exhausting it with the blocking peptide. These treatments abolished all immunolabeling (data not shown). In order to obtain unbiased data suitable for quantitative analysis, treatment groups were processed in a strictly parallel manner. Each group of treatments (such as 2-h treatments) had its own vehicle-controlled group, and brains belonging to the same treatment group were randomized and processed together for immunohistochemistry.

For immunoperoxidase staining, brain sections were permeabilized in 0.5% Triton X100 in 0.1 M PB for 1 h. Endogenous peroxidases were quenched with 3% H_2O_2 in 0.1 M PB for 15 min. Blocking of nonspecific labeling was made in 10% normal goat serum in 0.1 M PB for 1 h before incubation with the C-Ter antibody, diluted 1:1000 in 0.1 M PB containing 0.2% normal goat serum and sodium azide, for 48 h at 4°C. Immunolabeling was revealed using the anti-rabbit Vectastain Elite ABC kit from Vector Laboratories, and the tissue bound peroxidase was visualized with DAB chromogen reaction [0.4 mg/mL 3,3′-diaminobenzidine (DAB), 0.003% H_2O_2 in 0.05 M Tris buffer pH 7.6] for a few minutes. DAB incubation times were strictly identical for all sections within each group of treatments.

For immunofluorescence staining, serial brain sections were incubated with C-Ter rabbit antibody (diluted at 1:1000) and with mouse anti-CCK antibody [HYB 345-02] (Abcam, ref: ab37274, diluted at 1:1000) or mouse anti-calbindin antibody [CB-955] (Abcam, ref: ab82812, diluted at 1:300) (Siegel et al. 2010) overnight at room temperature in PBS (0.02 M) containing 0.3% Triton and 0.02% sodium azide (PBS-T-azide). Following washes, sections were incubated in Alexa Fluor® 488 anti-rabbit IgG and Alexa Fluor® 568 anti-mouse IgG (Invitrogen) diluted 1:1000 in PBS (0.02 M) containing 0.3% Triton (PBS-T) for 2 h at room temperature.

For CB1/MAP2 double labeling, brain sections of 1 CP-treated rat were incubated with rabbit C-Ter antibody (diluted at 1:1000) and with the mouse anti-MAP2 antibody (Sigma; diluted at 1:500) overnight at room temperature in PBS-T-azide. Following washes, sections were incubated in Alexa Fluor® 568 anti-rabbit IgG and Alexa Fluor® 488 anti-mouse IgG (Invitrogen) diluted 1:1000 in PBS-T for 2 h at room temperature.

Imaging and Quantification

Images of labeled rat brain sections were taken on a Zeiss AxioImager M1 microscope using a 20× numerical aperture (NA) 0.75 objective. In each experiment, all acquisitions were performed using strictly identical exposure conditions. For the MAP2 colocalization experiment, images were taken on a Nikon A1 laser-scanning confocal microscope with an oil-immersion 60×, NA 1.4 objective.

In immunoperoxidase experiments, cell bodies containing at least 5 labeled vesicles were unilaterally counted on 3 consecutive sections (150 μm total thickness) in the frontoparietal motor and somatosensory cortex and in the dorsal part of the hippocampus 3.3-mm caudal to the Bregma (Supplementary Fig. 1*A*). Results were expressed for each condition and each brain region as the average of labeled perikarya per animal ± standard error of the mean (SEM).

In immunofluorescence experiments, the number of CB1R-immunoreactive cells and the proportion of CB1-CCK and CB1-calbindin positives neurons were determined in the primary somatosensory cortex (hindlimb part) and in the anteromedial region of hippocampus (CA1 area) in all groups of animals (Fig. 4*C*). In the somatosensory cortex, quantification was performed in the different layers of cortex: layers I, II–III, IV, V, and VI. For the hippocampus, the CA1 area was divided in 4 layers: LMol (lacunosum moleculare), Rad (radiatum cell layer), Py (pyramidal cell layer), and Or (oriens layer). Positive cell bodies were unilaterally counted on 4 nonconsecutive sections (80-μm total thickness). Results were expressed for each condition and each brain region as the average number of labeled neurons per animal ± SEM.

For densitometry of CB1R immunofluorescent label analysis, we used ImageJ (http://rsb.info.nih.gov/ij/) to extract images and

measurements. After removal of background immunolabeling by subtracting mean density of the internal capsule, which in our conditions did not present any labeling, we measured the mean intensity of fluorescent labeling on a representative part of the superficial laminae of the somatosensory cortex (hindlimb part), the radiatium layer of CA1 area of the hippocampus and the pallido-nigral pathway, on 4 sections in 4 control animals and 3 CP 3*x*+ 2 h-treated animals. Results were expressed for each condition and each brain region as mean fluorescent intensity ± SEM in arbitrary units (mean grayscale pixel value).

Preembedding Immunoelectron microscopy

Brain slices were cryoprotected overnight at 4°C in 25% sucrose, 10% glycerin in 0.1 M PB. For permeabilization, sections were placed in an aluminum basket that was floated twice for 2 s on liquid nitrogen. Endogenous peroxidases were quenched with 3% H_2O_2 in 0.1 M PB for 15 min. Blocking of nonspecific labeling was made in 10% normal goat serum in 0.1 M PB for 1 h before incubation with the C-Ter antibody (diluted 1:1000 0.1 M PB containing 0.2% normal goat serum and sodium azide), for 48 h at 4°C. Immunolabeling was revealed by overnight incubation in ultra-small gold conjugate $F(ab')_2$ fragments of goat anti-rabbit IgG (Aurion, Netherlands, 1:100) at 4°C, followed by extensive washings, 10 min of postfixation in 2% glutaraldehyde and, finally, silver enhancement using the Aurion R-Gent SE-ME kit. Sections were osmificated with 1% osmium tetroxide in 0.1 M PB for 10 min, then with 0.5% osmium tetroxide for 20 min at room temperature, and dehydrated through increasing ethanol concentrations and propylene oxide. Sections were pre-embedded in propylene oxide/Durcupan (Durcupan ACM; Electron Microscopy Sciences) and flat embedded in fresh Durcupan onto quick-release-coated slides (Hobby Time Mold Parting Compound; Electron Microscopy Sciences), which were then covered with quick-release-coated coverslips and polymerized at 60°C for 24 h. Slides were evaluated with a light microscope to verify that CB1R distribution corresponded to the predominant distribution pattern detected in similarly treated animals (see above). Slides from selected animals were removed from the slide/coverslip, and areas of the Durcupan film containing areas of interest were cut out, re-embedded in Durcupan capsules, and polymerized for 24 h at 60°C. Ultrathin 45-nm serial sections were made on an ultramicrotome (Reichert-Jung Ultracut E), collected on Formvar-coated single slot grids, and stained with 1% uranyl acetate in 70% ethanol for 3 min and lead citrate for 2 min. Finally, the ultrathin sections were evaluated with a 1200EX electron microscope (JEOL Europe, Croissy sur Seine, France).

Western Blotting

Two hours after the end of the behavioral study, rats were deeply anaesthetized with pentobarbital (60 mg/kg i.p.) (Ceva Santé Animale, Libourne, France) and decapitated. A slice of the brain was realized from Bregma −1 mm to Bregma −4.5 mm and the hippocampus and neocortex, left and right, were dissected, pooled and immediately frozen in dry ice. Tissues were kept at −80°C until homogenization. Samples were homogenized on ice in 0.5 mL lysis buffer [1% n-dodecyl-beta-D-maltoside (Calbiochem), 100 mM NaCl, 20 mM TRIS-HCl (pH 7.4), 1 μM of phenanthroline and protease inhibitor mixture (Complete EDTA-free from Roche)] and placed for 30 min on a rotating wheel at 4°C. Insoluble material was removed by centrifugation at 30 000 × *g* for 30 min at 4°C. The protein concentrations were determined using a BCA Protein Assay Kit (Pierce, UK). Proteins were separated by 10% sodium dodecyl sulfate polyacrylamide gel electrophoresis and transferred to a nitrocellulose membrane. Blots were probed with CB1R C-terminal antibody (1:1000) and beta-actin antibody (1:100 000 from Abcam) for loading control. Blots were then incubated with HRP-conjugated secondary antibodies (1:10 000; GE Healthcare) followed by Supersignal® West Pico Chemiluminescent Substrate (Pierce). Immunoreactive bands were quantified using ImageJ.

Statistical Analysis

Student *t*-test or 1-way analysis of variance followed by Student–Newman–Keuls test was performed using SigmaStat software to test for the statistical significance of the results, when appropriate.

Results

Steady-State Distribution of CB1R in Selected Forebrain Areas

At the investigated forebrain level (Supplementary Fig. 1*A*), the purified anti-CB1R antibody produced strong labeling of the neocortex, the hippocampal formation, the pallido-nigral pathway of the basal ganglia and the basolateral complex of the amygdala. This distribution is fully coherent with recent reports (Katona et al. 1999, 2001; Tsou et al. 1999; Egertova and Elphick 2000; Morozov and Freund 2003; Bodor et al. 2005; Matyas et al. 2006), which, by using comparable experimental conditions, reported a high level of CB1R expression in a subset of GABAergic neurons in these brain regions. Since the above studies provide high-quality data down to the ultrastructural level, in the present report we specify only certain features of steady-state CB1R distribution, which are directly relevant to the subject of the present study, by focusing our analysis to the less well-studied somatodendritic region of CB1R-expressing neurons.

In the neocortex and hippocampus, intense staining was localized to a dense network of highly branched and beaded axons in a characteristic laminar pattern (Fig. 1*A*) as well as to the somatodendritic compartment of sparse neurons, where it appeared as puncta (Fig. 1*B*). In the neocortex, the majority of stained axons and cell bodies were found in layers II–III, and VI. In the hippocampal formation, labeled somata were found mainly in the stratum radiatum in CA1 and CA3 fields and in the molecular layer of the dentate gyrus, while a dense plexus of stained axons was found in all layers. In the pallido-nigral pathway the labeling was confined to a fine meshwork of thin and varicose-less axons (illustrated in Fig. 5).

In order to characterize the CB1R-immunoreactive somatodendritic puncta, we analyzed the perikarya of CB1R-immunoreactive hippocampal interneurons by electron microscopy, mostly from the dentate gyrus, where a relatively high density of CB1R expressing neurons facilitates ultrastructural observation. CB1R-immunoreactive neurons were characterized by an electrolucent cytoplasm containing a well-developed smooth ER and a large invaginated nucleus with a prominent nucleolus (Fig. 1*C*), further confirming that CB1Rs are expressed mostly in interneurons (Leranth et al. 1984; Acsady et al. 1996). In the somatodendritic region, around one-third of immunogold particles were localized to intracellular organelles, often showing complex, membranous intraendosomal morphology (Fig. 1*D,E*). A relatively small proportion of gold particles were localized on the somatodendritic cell membrane, the rest being intracellular, nonendosomal receptors, localized to the Golgi apparatus, the endoplasmic reticulum or to nonidentified structures (Fig. 1*D*). Immunogold particles detecting the cytoplasmic C-terminal of the CB1R were almost exclusively localized to the cytoplasmic surface of organelles, showing that CB1Rs are localized to the limiting membrane (Fig. 1*D,E*).

Agonist and Antagonist/Inverse Agonist Treatment Inversely Regulates Somatodendritic CB1R Localization

Treatment with synthetic cannabinoid ligands resulted in a striking redistribution of CB1Rs in neurons (Fig. 2 and Table 1). Two hours after injection of agonist CP55 940, the number of neuronal perikarya containing CB1R-immunopositive vesicles

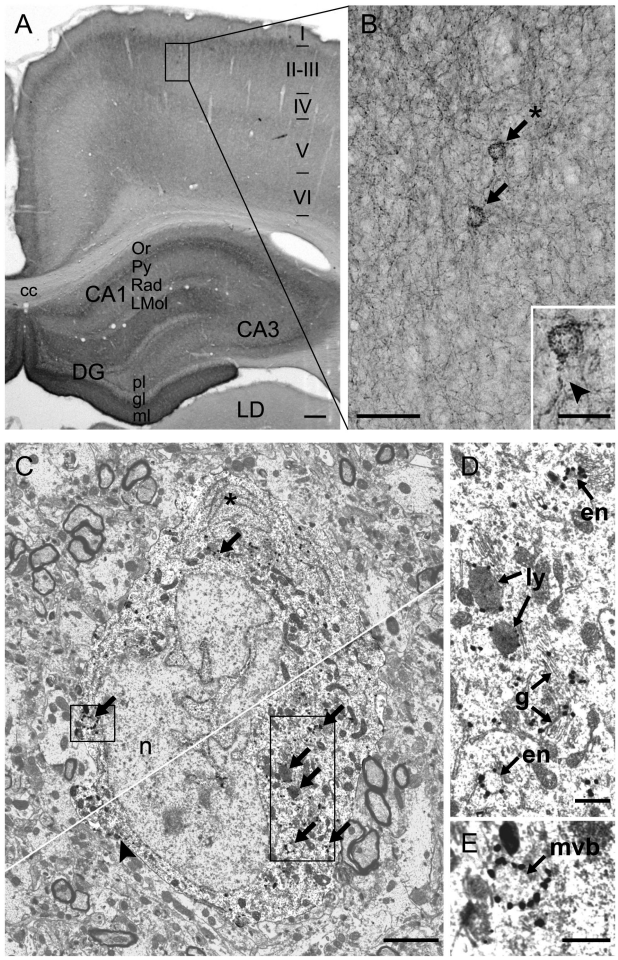

Figure 1. Steady-state distribution of CB1R in rat neocortex and hippocampus. (*A*) CB1R immunopositive axons and perikarya are distributed in a characteristic laminar pattern in the hippocampus and the somatosensory fronto-parietal cortex. (*B*) Higher magnification of 2 layer II cortical neurons (arrows) shows characteristic vesicular labeling in the perikaryon and occasionally in proximal dendrites (arrowhead). The inset shows higher magnification of the neuron labeled with an asterisk. I–VI, cortical layers I–VI; cc, corpus callosum; LMol, lacunosum moleculare; Rad, radiatum cell layer; Py, pyramidal cell layer and Or, oriens layer; ml, molecular layer; gl, granular layer; pl, plexiform layer; LD, lateral dorsal nucleus of the thalamus. (*C*) Ultrastructural analysis of a representative CB1R immunolabeled interneuron from the hippocampal dentate gyrus shows a characteristic invaginated nucleus (n), a relatively electrolucent cytoplasm with eminent smooth endoplasmic reticulum (asterisk) and CB1R immunolabeling in intracellular organelles (thick arrows) and on the somatodendritic cell membrane (arrowhead). (*D–E*) Higher magnification view of 2 regions (boxed on C) shows immunolabeling in endosomes (en), in multivesicular-body-like structures (mvb), in the Golgi apparatus (g) and in lysosomes (ly, thin arrows). Gold particles labeling CB1Rs are located on the cytoplasmic side of the endosomal membranes, coherent with the localization of the C-terminus of CB1R. The difference in size of the gold particles is due to silver amplification. Scale bars, 200 μm on (*A*), 50 μm on (*B*), 20 μm on the inset of (*B*), 2 μm on (*C*), and 500 nm on (*D*, *E*).

increased (Fig. 2*B*) by approximately 300% in the hippocampus and 270% in the neocortex (Fig. 2*D*). This effect was prolonged to 16 h after injection in the hippocampus, with still significantly higher number of labeled neurons than in control (i.e. vehicle-injected) animals, whereas the amount of labeled perikarya in the neocortex returned to control level; this demonstrates that the effect of agonist treatment is reversible, but it follows different kinetics in the hippocampus and the neocortex (Fig. 2*D*). Electron microscopic observation suggested that the highly significant elevation of somatodendritic labeling is a result of translocation of CB1Rs to intracellular organelles, as shown by numerous gold particles localized to somatic endosome-like intracellular organelles (Fig. 2*F*, inset).

In marked contrast to the agonist treatment, injection of the antagonist/inverse agonist AM251 resulted in a notable decrease in somatic endosomal labeling (Fig. 2*C*) down by about 33% of the control values both in the hippocampus and the neocortex, at 2 h after treatment (Fig. 2*E*). As the time-course for antagonist/inverse agonist-mediated externalization is relatively slow compared with agonist-mediated internalization in transiently transfected HEK-293 cells (Leterrier et al. 2004), we also measured the number of perikarya displaying endosomal CB1R staining 4 h after acute antagonist/inverse agonist treatment. At this time point, the reduction in labeled perikarya reached around 60% both in the hippocampus and in the neocortex (significantly lower than at the 2 h time point), and electron microscopic observation indicated that at least a portion of CB1Rs were inserted in the somatic cell membrane (Fig. 2*G*, inset). Interestingly, 16 h after AM251 treatment the number of labeled somata returned to control values both in the hippocampus and in the neocortex.

These results support that, similar to in vitro findings (Hsieh et al. 1999; Jin et al. 1999; Coutts et al. 2001; Leterrier et al. 2004, 2006), acute agonist treatment also results in a significant internalization of CB1Rs in vivo, while inverse agonist treatment leads to a reversible decrease of basal CB1R endocytosis.

Acute Agonist Treatment Leads to Appearance of CB1R Containing Endosomes in Axon Terminals

Electron microscopic observation of axon terminals in the molecular layer of the hippocampal dentate gyrus has shown that, in control animals, the majority of CB1Rs localize to the axonal cell membrane of symmetric synapses and axon shafts (Fig. 3*A*). The density of CB1Rs was consistently higher in axon shafts than in terminals, indicating a predominantly extrasynaptic cell membrane localization of axonal CB1Rs, similarly to previous in vitro (Leterrier et al. 2006) and in vivo (Bodor et al. 2005; Nyiri et al. 2005; Matyas et al. 2006) reports. Notably, 2 h after treatment with agonist CP55 940, the occurrence of presynaptic profiles containing gold particles localized to intracellular organelles increased (Fig. 3*B–D*). In axon shafts, the gold particles conserved a predominant localization at the cell membrane, but occasionally CB1R-immunopositive endosomes were also observed (Fig. 3*B–D*). In conclusion, at steady state, the predominant localization of axonal CB1Rs is on extrasynaptic cell membrane. Agonist treatment for 2 h likely leads to a partial internalization of axonal CB1Rs, predominantly in axon terminals, while in axon shafts CB1Rs remain mostly on the cell membrane.

Repeated Agonist Treatment Leads to Region-specific Translocation of Axonal CB1Rs

As a single agonist treatment resulted only in a partial internalization of axonal CB1Rs, we repeated the agonist injection during 3 consecutive days and investigated CB1R distribution 2 h after the last treatment. At this time point, significant tolerance developed against the analgesic and cataleptic effects of CP55 940 (Fig. 4*A*,*B*). Light microscopy analysis showed dramatic redistribution of CB1Rs in the neocortex and

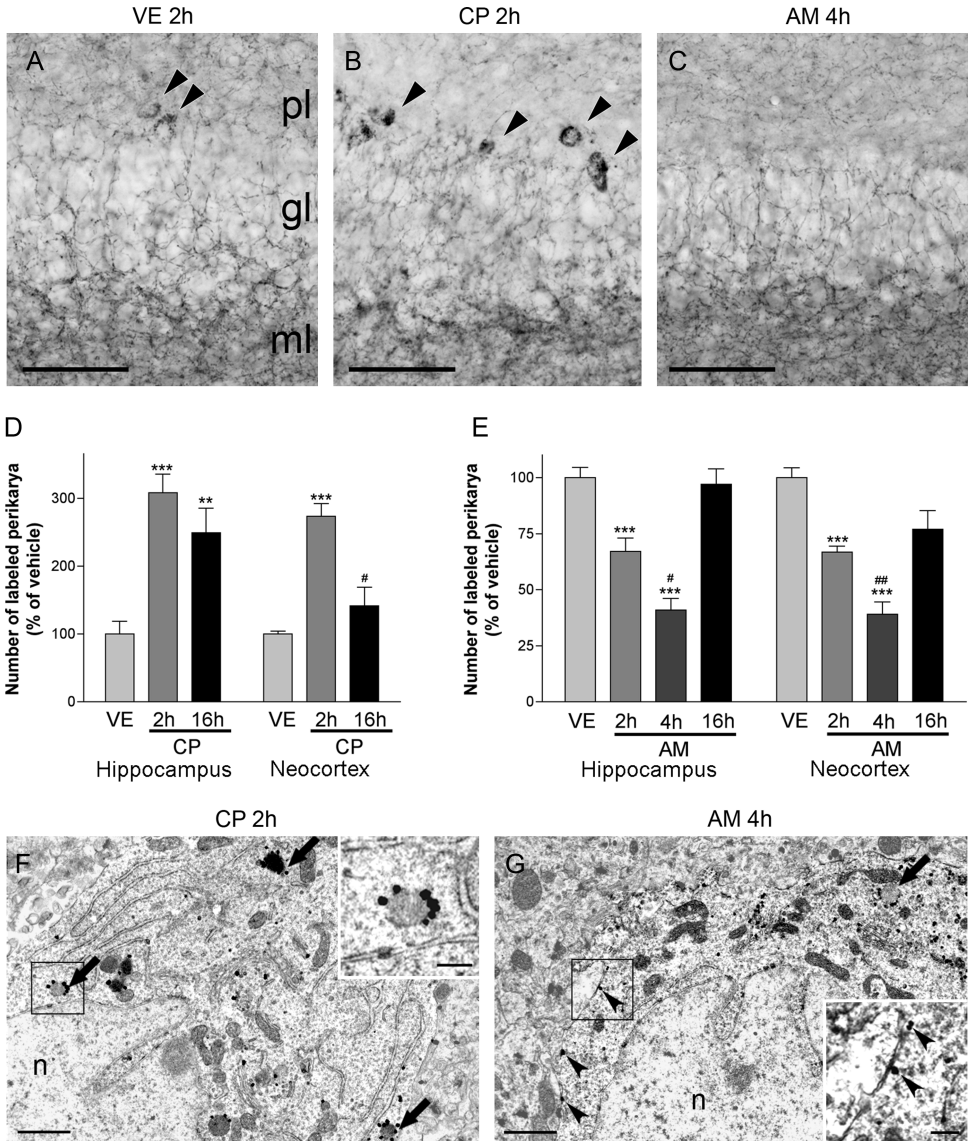

Figure 2. Agonist and inverse agonist treatments have opposite effects on subcellular localization of CB1R in the neocortex and hippocampus. (*A–C*) Representative images showing the effects of acute vehicle (*A*), agonist (*B*), and inverse-agonist (*C*) treatment on the distribution of CB1R in the dentate gyrus. Acute agonist treatment (*B*) results in a significant increase in the number of perikarya containing CB1R-positive endosomes after 2 h both in the neocortex and in the hippocampus (*D*). Inverse agonist treatment (*C*) results in significantly lower number of labeled perikarya both in the neocortex and in the hippocampus (*E*), and this effect is more pronounced 4 than 2 h after treatment. Sixteen hours after treatment, most values approached control levels. (*F*) Representative electron microscopic image of a neuron from the dentate gyrus 2 h following CP55 940 treatment, displaying numerous CB1R-immunolabeled intracellular organelles (arrows). (G) Electron microscopic image of a neuron from the dentate gyrus following 4 h AM251 treatment, displaying a residual CB1R labeled endosome (arrow) and several gold particles labeling CB1Rs on the cell membrane (arrowheads). Insets in (*F, G*) show higher magnification of boxed regions. pl, plexiform layer; gl, granular layer; ml, molecular layer; VE, vehicle; CP, agonist CP55 940; AM, inverse agonist AM251. Values represent the mean percentages of vehicle ± SEM. $^{*}P < 0.05$; $^{**}P < 0.01$; $^{***}P < 0.001$ as compared with control. $^{\#}P < 0.05$ and $^{\#\#}P < 0.01$ as compared with 2 h. Scale bars: 50 μm on (*A–C*), 1 μm on (*F, G*), and 250 nm on the insets of (*F, G*).

Table 1
CB1R labeled perikarya in the fronto-parietal cortex and dorsal hippocampus of rats after different pharmacological treatments

	Neocortex			Hippocampus		
	Single-dose + 2 h ($n = 4$)	Single-dose + 4 h ($n = 3$)	Single-dose + 16 h ($n = 3$)	Single-dose + 2 h ($n = 4$)	Single-dose + 4 h ($n = 3$)	Single-dose + 16 h ($n = 3$)
Vehicle	89 ± 5.3	63 ± 4.4	126 ± 4.2	41 ± 1.9	44 ± 2.0	68 ± 12.7
CP55 940	241 ± 27.9***	ND	179 ± 43.1	126 ± 11.1***	ND	170 ± 29.7**
AM251	64 ± 5.7***	35 ± 3.5***	97 ± 12.7	27 ± 2.5***	18 ± 2.3***	66 ± 5.7

Rats received a single dose of vehicle, agonist CP55 940, or inverse agonist AM251 and were sacrificed 2, 4, or 16 h after the injection. Perikarya were counted in dorsal hippocampus (Hc) and neocortex (Cx) on 3 consecutive 50 μm thick sections (total thickness = 150 μm), as indicated on Supplementary Figure 1. Results are mean ± SEM. ND, not determined.
$^{**}P < 0.01$; $^{***}P < 0.001$ as compared with control.

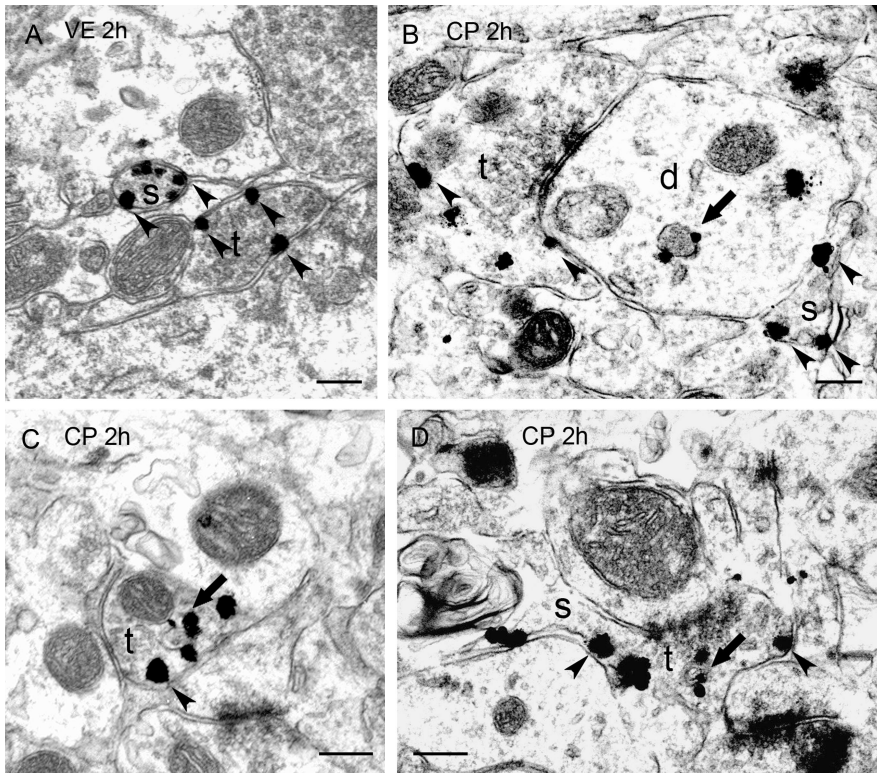

Figure 3. Acute agonist treatment leads to appearance of CB1R containing endosomes in axon terminals. (*A*) In the dentate gyrus, in vehicle-treated control animals, gold particles labeling CB1Rs are localized mainly to the cell membrane (arrowheads) of preterminal axon segments or axon shafts (s) and to a lesser degree to inhibitory terminals (t), which were identified by the presence of symmetric synapses and small synaptic vesicles. (*B–D*) Acute agonist treatment (2 h CP55 940) results in partial internalization of CB1Rs (arrows) mainly in terminals, as indicated by endosomal localization of gold particles. On (*B*) the inhibitory terminal (t) establishes a synapse with a dendrite (d) containing a labeled endosome (arrow). Scale bars: 200 nm.

hippocampus. First, we observed a significant increase in the number of CB1R immunoreactive cell bodies, both by immunofluorescence (Fig. 4*D–G*) and by immunoperoxidase labeling (Supplementary Fig. 2*A*,*B*,*E*). Labeled neurons displayed a marked vesicle-like labeling, which often completely filled the cytoplasm and proximal dendrites (Fig. 4*E,* inset and Supplementary Fig. 2*C,D*), as confirmed by the colocalization between CB1R immunoreactivity and the somatodendritic marker MAP2 labeling on a thin equatorial confocal section (Fig. 4*H*). This effect was a result of pharmacological CB1R activation, since it could be abolished through co-administration of AM251 (Fig. 4*D–G* and Fig. 6*D*,*E*). Strikingly, in contrast to effects measured 2 h after a single CP55 940 treatment, this redistribution also resulted in a significant decrease in CB1R axonal labeling intensity (Fig. 5*F*). CB1R protein levels were also highly decreased in both regions (Fig. 4*I* for the hippocampus and data not shown for the neocortex). Interestingly, this redistribution was not found in all CB1R-expressing regions in the forebrain. Indeed, axonal labeling density was unchanged in extrapyramidal tracts such as the pallido-nigral pathway (Fig. 5*A*,*E*,*F*). Accordingly, in corresponding somata, vehicle-treated animals exhibited very weak nonvesicular somatodendritic labeling in the central part of the striatum (similar to previous findings; Matyas et al. 2006), which did not change noticeably in agonist-treated (CP 2 h and CP 3 × + 2 h) animals (data not shown).

Although the number of labeled perikarya increased in the hippocampus and in the neocortex after repeated agonist treatment, quantification demonstrated that there was no change in the laminar localization of labeled cell bodies which are characteristic to the CB1R-expressing interneuron subtypes described previously (Katona et al. 1999, 2001; Tsou et al. 1999; Egertova and Elphick, 2000; Morozov and Freund 2003; Bodor et al. 2005; Matyas et al. 2006). Indeed, after CP55 940 treatment, the increase in CB1R immunoreactive cell bodies occured in the radiatum layer of the hippocampus and in the laminae II–III and VI of cortex, where the majority of CB1R positive perikaria was observed in control animals (Fig. 4*F*,*G*).

According to a previous characterization in untreated animals, CB1R-positive neurons in the neocortex are mainly either cholecystokinin (CCK)- or calbindin-expressing interneurons (Bodor et al. 2005). Thus, we analyzed the identity of neurons filled by CB1R-immunoreactive endosomes after CP55 940 treatment in double immunostaining experiments using these 2 markers (Fig. 6*A–C*). In the somatosensory cortex, we observed that cells accumulating CB1R-immunoreactive vesicle-like labeling in response to pharmacological stimulation are principally CCK-positive neurons (Fig. 6*D* and Supplementary Table 1). The number of CB1R/CCK-positive perikarya was significantly up-regulated compared with control at the end of CP55 940 treatment, while the number of CB1/calbindin-positive neurons was unchanged (Fig. 6*D*). In the CA1 area of the hippocampus, we found similar results, the neurons accumulating CB1R were principally CCK-positive (Fig. 6*E* and Supplementary Table 2). Importantly, in both analyzed regions, the numbers of CCK- and calbindin-positive neurons were not modified by

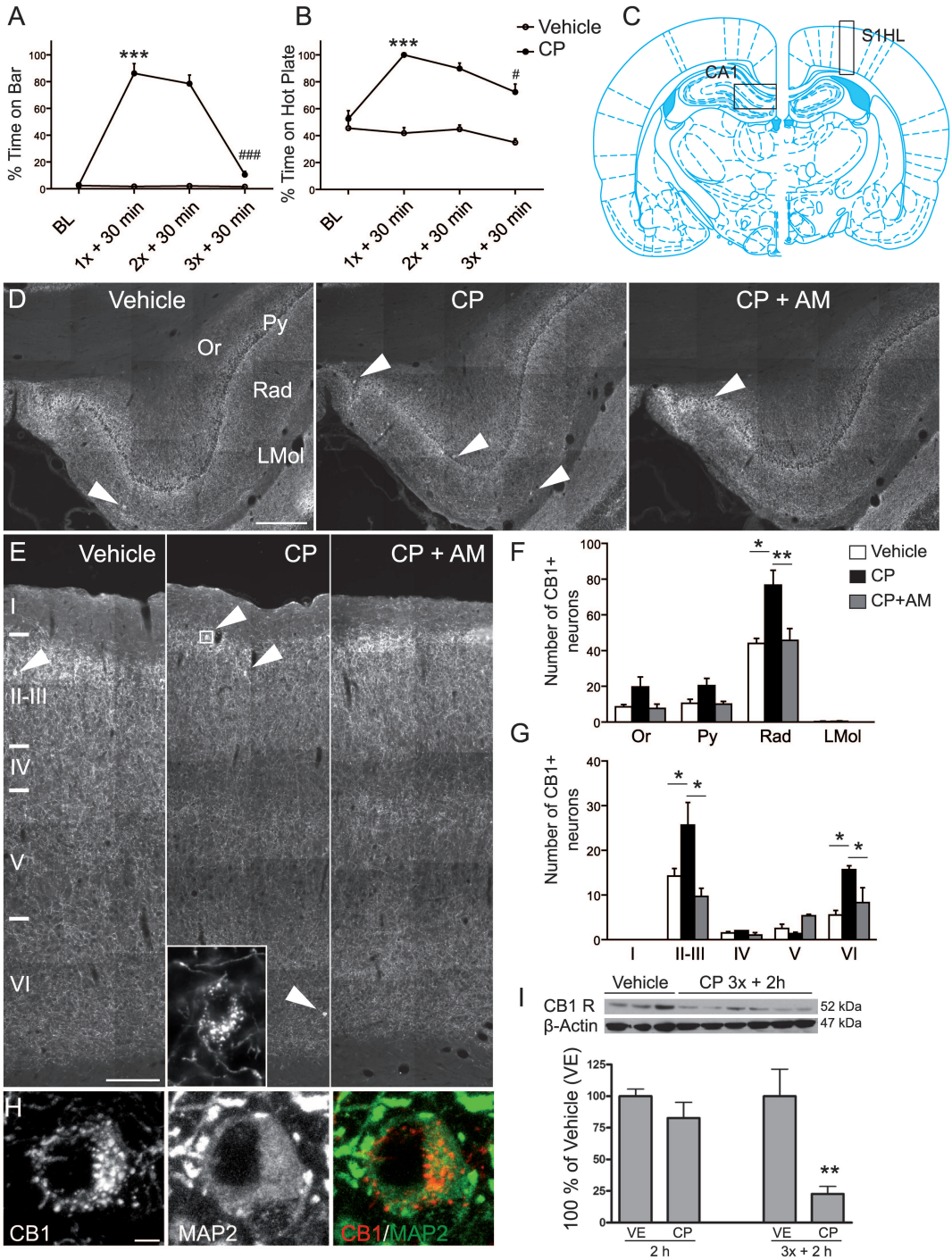

Figure 4. Sustained agonist treatment leads to significant up-regulation of the number of CB1R-positive neurons in the hippocampus and primary somatosensory cortex. (*A*, *B*) Repeated agonist treatment ("CP 3*x* + 2 h" for CP55 940 treatment repeated during 3 consecutive days with fixation at 2 h after the last treatment) results in a significant tolerance developed against the cataleptic (*A*, bar test) and analgesic (*B*, hot plate test) effects of CP55 940. Tests were performed before the first treatment (BL for baseline), then 30 min after each daily treatment during 3 days. Values were expressed as mean ± SEM; $^{***}P < 0.001$ as compared with BL; $^{\#}P < 0.05$ as compared with 1*x* + 30 min and $^{\#\#\#}P<0.001$ as compared with 1*x* + 30 min. (*C*–*G*) Chronic treatment leads to a significant increase in the number of CB1R-labeled perikarya in the radiatum layer of the hippocampus (*D*, *F*) and in the laminae II–III and VI of cortex (*E*, *G*). Arrowheads in (*D*, *E*) show labeled perikarya in each condition. Inset in (*E*): higher magnification image of 1 representative cell from layers II–III of the somatosensory cortex where cell body and proximal dendrites are filled with CB1R immunoreactive endosomes. Quantification was realized on the CA1 area of the hippocampus and on the primary somatosensory cortex (Hindlimb part) as illustrated in (*C*) (black squares). Or, oriens layer; Py, pyramidal layer; Rad, radiatum layer; LMol, lacunosum moleculare. (*H*) Colocalization between CB1R immunoreactivity and somatic MAP2 labeling (MAP2 labeling is very strong in dendrites and strong-moderate in soma), shown on this thin equatorial confocal optical section, indicates the somatodendritic localization of CB1R immunoreactive endosomes. (*I*) Representative example of a western blot for CB1R and β-actin in vehicle and chronic CP55 940-treated rat in hippocampus. Densitometry analysis of the CB1R protein expression normalized to β-actin protein expression shows a statistically significant decreased expression of CB1R induced by the CP55 940 treatment only after 3 days of treatment but not at 2 h after a single treatment ($^{**}P < 0.01$). Data were expressed as mean percentage to control values (vehicle) ± SEM. Scale bars: 200 μm on (*D*), (*E*) and 5 μm on (*H*).

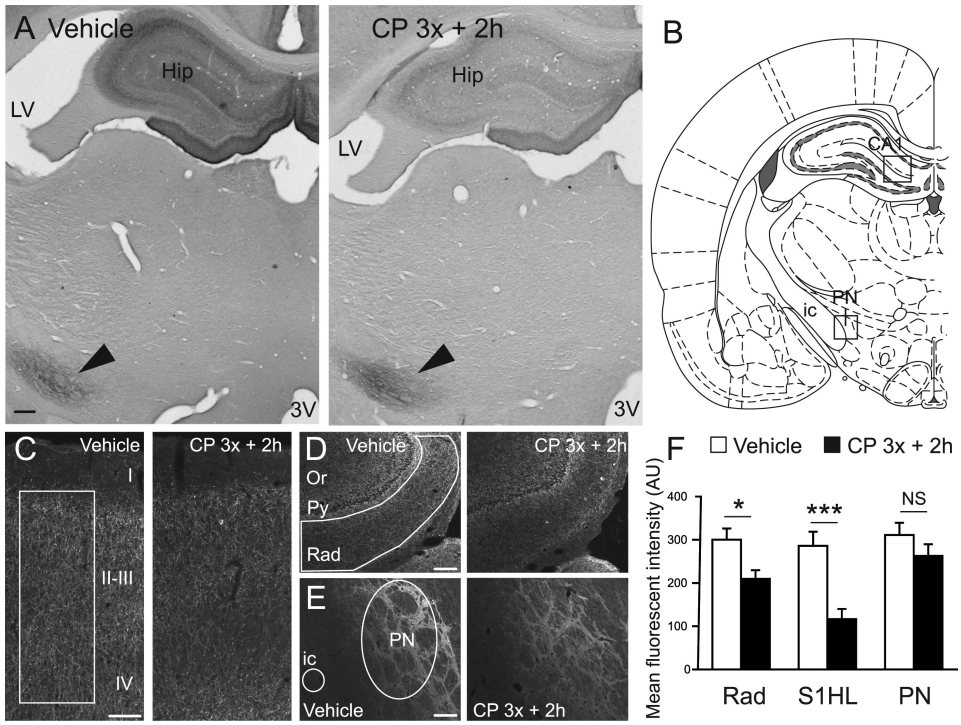

Figure 5. Sustained agonist treatment leads to region-specific down-regulation of axonal CB1R. (*A*) CB1R immunoreactivity in the hippocampus (Hip) is down-regulated after repeated agonist (CP 3 x + 2 h) treatment, as compared with vehicle, while labeling intensity remains elevated on the same section in the pallido-nigral pathway of the basal ganglia (arrowheads). (*C–E*) Representative example of CB1R immunofluorescent staining in the primary somatosensory cortex (hindlimb part, S1HL) (*C*), in the CA1 part of hippocampus (*D*, boxed on *B*) and in the pallidro-nigral pathway (*E*, boxed on *B*) in a representative vehicle (left panel) and CP-treated rat (right panel). Selected regions of interest (indicated by white selections on *C*, *D*, and *E*) were used to measure the mean fluorescence intensity. Fluorescence intensity of the internal capsule (ic) was used for background. (*F*) Densitometry reveals that repeated CP treatment significantly decreases mean CB1R fluorescence intensity in hippocampus (radiatum layer of the CA1 region, Rad), primary somatosensory cortex (S1HL) but not in the pallido-nigral pathway (PN). Results are expressed as mean intensity ± SEM in arbitrary units (AU). ***$P < 0.001$ and *$P < 0.05$ as compared with vehicle. 3V, third ventricle; LV, lateral ventricle. Scale bars, 200 μm on (*A*) and 100 μm on (*C–E*).

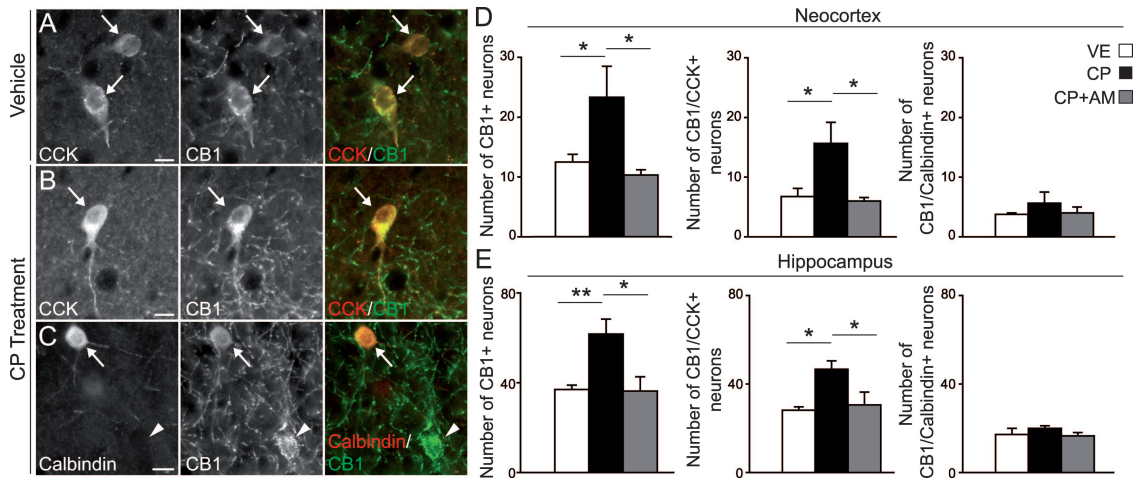

Figure 6. Sustained agonist treatment leads to accumulation of CB1R mostly in cell bodies of CCK-positive interneurons in hippocampus and primary somatosensory cortex. (*A, B*) Double immunofluorescent staining for CB1R (green) and CCK (red) in the somatosensory cortex after control (*A*) or repeated agonist (*B*) treatment. CB1R/CCK double-labeled cells are shown by arrows. (*C*) Double immunofluorescent staining of CB1R (green) and calbindin (red) in the somatosensory cortex in a CP55 940-treated animal. Arrows point to a CB1R/calbindin double-labeled cell and arrowheads to a calbindin-positive cell devoid of CB1R labeling. (*D* , *E*) Number of cell bodies immunoreactive for CB1R (left), CB1R and CCK (middle), or CB1R and calbindin (right), after control, CP55 940, or CP55 940 + AM251 repeated treatments in the hindlimb part of the somatosensory cortex (*D*) and the CA1 area of the hippocampus (*E*). Chronic treatment with agonist CP55 940 leads to a significant increase in the number of CB1R labeled perikarya in both regions, principally in CCK-positive interneurons. The number of double-labeled CB1R/calbindin-positives cells is unchanged at the end of the treatment. CP55 940 + AM251 treatment has no effect on the number of positive cells and on their neurochemical identity. Results are expressed as mean number ± SEM. **$P < 0.01$ and *$P < 0.05$. Scale bars: 10 μm.

CP55 940 treatment (Supplementary Fig. 3*A–D*). Even though we cannot formally exclude that a new subpopulation of CCK-positive interneurons may start expressing CB1R after repeated CP55 940 treatment, the above results strongly suggests that the increase in number of cell bodies with CB1R immunoreactivity after repeated CP55 940 treatment is due to

a redistribution of CB1R from axons of neurons that already express CB1R at steady state.

In conclusion, repeated agonist treatment leads to development of tolerance against the analgesic and cataleptic effects of CP55 940, as well as to a significant redistribution of axonal CB1Rs in all forebrain regions investigated, with the exception of the basal ganglia.

Discussion

Steady-State Distribution of CB1R

In control animals, we observed a high level of axonal immunolabeling, accompanied by labeling of somatodendritic endosomes in interneurons. In axons, CB1Rs were localized to the membrane of axon shafts (or preterminal axons) and to a lesser degree to the membrane of synaptic varicosities and terminals. A relatively low but consistent proportion of receptors was also found at the somatodendritic cell membrane. These findings are consistent with recent high-resolution data reported using other antibodies (Bodor et al. 2005; Nyiri et al. 2005; Kawamura et al. 2006; Matyas et al. 2006), and are also in accordance with the distribution previously reported in vitro for both endogenous and transfected CB1Rs in cultured primary hippocampal neurons (Leterrier et al. 2006).

Notably, our experimental protocol, which was aimed to obtain a high signal-to-noise ratio detection of CB1Rs expression in interneurons, did not detect the recently reported expression of CB1Rs in principal hippocampal neurons (Katona et al. 2006; Kawamura et al. 2006), which is at least an order of magnitude lower than in GABAergic neurons (Kawamura et al. 2006). Thus, results of the present study relate to the major, readily detectable population of CB1Rs expressed by GABAergic neurons in the hippocampus, neocortex and basal ganglia (Freund et al. 2003).

Agonist Treatment Results in Region-specific Internalization of CB1Rs

Acute treatment with agonist CP55 940 induced CB1R internalization, as indicated by the 2-fold increase in the number of perikarya containing CB1R-immunoreactive vesicles. Ultrastructural analysis suggested that the increase of somatodendritic labeling is a result of CB1R translocation to endosomes. Comparable in vivo effects of acute agonist administration have been reported for several GPCRs such as SST_{2A} somatostatin (Csaba et al. 2001), M2 muscarinic (Bernard et al. 1998), and 5-HT_{1A} serotonin receptors (Riad et al. 2004). Interestingly, near-maximal increase in the number of labeled perikarya 2 h after agonist treatment was not accompanied by significant decrease of axonal labeling, which required repeated, daily agonist treatments even in the most responsive regions, such as the neocortex and hippocampus. It is likely that the small fraction of CB1R internalized from the highly branched axonal arbors of CCK-containing interneurons at 2 h is sufficient for labeling the perikarya of nearly all CB1R expressing neurons and that endosomes containing endocytosed axonal CB1Rs during sustained activation further fill up the perikarya and proximal dendrites of the same neurons. It is also remarkable that, at 16 h after a single treatment, the number of labeled perikarya returns near to control levels in the neocortex, whereas the same treatment repeated at 24 and 48 h after the first treatment results in a very significant net diminution of axonal CB1Rs. CB1Rs are efficiently recycled after moderate activation, as described previously in vitro (Rinaldi-Carmona et al. 1998; Hsieh et al. 1999; Leterrier et al. 2004); however, more sustained activation redirects CB1Rs to alternative intracellular routes, such as the activation-level dependent GASP1-mediated CB1R degradation pathway (Martini et al. 2006), leading to the characteristic down-regulation reported to parallel the development of tolerance. However, the relationship between CB1R internalization and tolerance is more complex since, on a shorter time-scale, efficient internalization leads to faster resensitization, possibly through more efficient dephosphorylation and recycling; this may explain why in vitro treatment with low endocytotic agonists such as Δ^9-THC leads to faster receptor desensitization and slower resensitization, as compared with high endocytotic agonists such as WIN55,212-2 or CP55 940 (Wu et al. 2008).

Retarded axonal translocation kinetics likely result from a slow internalization rate of axonal CB1Rs. Indeed, previous in vitro results (Coutts et al. 2001; Leterrier et al. 2006) indicate that agonist-induced internalization of CB1R in axons of mature cultured neurons requires 16 h of continuous agonist treatment for completion. In contrast, HEK-293 cells or other heterologous expression systems reach the maximal level of endocytosis after only 15–30 min (Rinaldi-Carmona et al. 1998; Hsieh et al. 1999; Leterrier et al. 2004), showing the relatively low efficacy of the axonal endocytotic machinery. Interestingly, high-resolution studies in cultured hippocampal neurons have demonstrated that endocytosis from the axonal cell membrane is restricted to nerve terminals and varicosities, whereas dendrites and immature axons are capable of internalization along their whole length (Sinclair et al., 1988; Parton et al. 1992; Parton and Dotti 1993), Thus, preterminal axons and axon shafts, where CB1Rs are concentrated (our present results and Bodor et al. 2005; Nyiri et al. 2005; Kawamura et al. 2006; Matyas et al. 2006) may not be favorable for internalization of activated CB1Rs, which may need to be transported to considerable distances to reach synapses and varicosities in order to access the endocytic machinery. In certain pathways of the basal ganglia, that express functional CB1Rs on thin, unmyelinated fibers devoid of synaptic specializations, such as the pallido-nigral and striato-pallidal projections (Matyas et al. 2006), this distance may reach several hundreds of micrometers. It is tempting to attribute the apparent lack of CB1R redistribution in pallido-nigral axons after prolonged agonist treatment, reported in this study, to their pronounced inability to internalize. Interestingly, basal ganglia display also very moderate down-regulation of CB1Rs following chronic exposure to Δ^9-THC or synthetic agonists in several studies, as compared with other brain regions (see Sim-Selley 2003; Gonzalez et al. 2005 for recent reviews). Considering GPCR endocytosis as the first step of receptor down-regulation, the present results suggest a simple mechanistic explanation for the marked region-specific differences in down-regulation of CB1Rs: the internalization and down-regulation of axonal CB1Rs is inversely proportional to the distance from potential internalization sites, such as terminals and axonal varicosities. Further studies with systematic comparative analyses of internalization patterns of CB1Rs in the basal ganglia are needed to confirm this hypothesis. In addition, for a better comprehension of region-specific differences in tolerance development, it is also necessary to better understand putative region-specific differences in CB1R

phosphorylation and dephosporylation patterns. Interestingly, the relatively reduced internalization capacity of the basal ganglia reported in this study also suggests an explanation for the reported lack of difference in desensitization between high and low endocytic agonists in the basal ganglia (Sim-Selley and Martin 2002): in the neocortex and hippocampus, efficient internalization, dephosphorylation, and recycling allow partial CB1R resensitization in animals treated with high, but not low, endocytotic agonists, while the basal ganglia mostly lacks this internalization-dependent resensitizing mechanism.

Constitutive Internalization Revealed by Antagonist/Inverse Agonist Treatment

In a striking contrast to agonist effects, acute treatment with the antagonist/inverse agonist AM251 resulted in a significant decrease of cell bodies showing a vesicular-like labeling for CB1R. This effect was also reversible, since 16 h after treatment, the number of labeled perikarya approximated the number observed in control animals. To our knowledge, comparable findings have never been reported for cerebral GPCRs. In our interpretation, the inverse-agonist-sensitive endosomal presence of CB1R at steady-state results from constitutive receptor internalization. This interpretation is based on previous findings from 2 different laboratories, which, by using transfected HEK-293 cells or cultured hippocampal neurons, reported an inverse-agonist sensitive constitutive endocytosis of CB1Rs (Leterrier et al. 2004; Ellis et al. 2006), which is important for the correct axonal targeting of newly synthesized CB1Rs (Leterrier et al. 2006). The existence of constitutive activation-dependent CB1R endocytosis was independently confirmed by a recent study (D'Antona et al. 2006), which studied the T210 residue of CB1R, which forms part of the "ionic lock," an electrostatic interaction between a triad of charged amino acids that tether cytoplasmic extremities of third and sixth transmembrane domains together to stabilize the inactive state of GPCRs (Kobilka and Deupi 2007). Structural analysis indicates that this "ionic lock" is weaker in wild-type CB1Rs than in most GPCRs (D'Antona et al. 2006), providing a molecular basis for its elevated propensity to adopt an active conformation. Notably, reinforcement of this "ionic lock" by mutating T210 to alanine diminishes constitutive activity and enhances cell membrane localization at steady state (D'Antona et al. 2006). In parallel to this structural determinant, basal activity of CB1Rs is also maintained by constitutive and cell-autonomous or paracrine production of endocannabinoids such as 2-arachidonoyl-glycerol (2-AG), as described recently both in CHO (Chinese Hamster Ovary) cells and in isolated cultured hippocampal neurons (Turu et al. 2007). Indeed, recent studies show that DAGLα, the synthesizing enzyme of 2-AG is selectively localized to the somatodendritic cell membrane in neurons (Katona et al. 2006; Yoshida et al. 2006; Uchigashima et al. 2007).

In conclusion, our results show that agonist-mediated internalization of CB1 cannabinoid receptors in vivo is readily detectable in most brain areas that were investigated, with the notable exception of the basal ganglia. We also show that although intracellular translocation following single-dose agonist administration is reversible, sustained agonist treatment leads to pronounced somatodendritic accumulation accompanied by receptor down-regulation. Thus, internalization of CB1Rs is likely one of the early pharmacodynamic adaptive mechanisms that lead to reduced responsiveness and tolerance in the case of prolonged or repeated activation. This interpretation stipulates that an increase in somatodendritic CB1R-labeling intensity is mostly due to intraneuronal translocations, and not to an increase in receptor synthesis. Indeed, CB1R protein levels were unchanged after acute agonist treatment; conversely prolonged treatment, which resulted in a maximal increase of somatodendritic labeling, was accompanied by a significant net decrease of CB1R protein levels. We also present evidence suggesting that steady state endocytosis of CB1Rs after antagonist/inverse agonist treatment results in a significant diminution of intracellular vesicular labeling. The presence of CB1Rs in intracellular vesicles, accompanied with an inverse-agonist-induced decrease of this endosomal label, suggests that a substantial proportion of CB1Rs is permanently activated, internalized, and recycled at steady state.

Supplementary Material

Supplementary material can be found at: http://www.cercor.oxfordjournals.org/.

Funding

This work was supported by grants from the "Centre National de la Recherche Scientifique" (CNRS) and Hungarian Scientific Research Fund (OTKA-K62893).

Notes

The authors thank J. Helfferich and D. Kézdy (Laboratory of Neuromorphology, Budapest, Hungary) for skillful technical assistance. They also thank C. Ledent (Université libre de Bruxelles, Bruxelles, Belgium) for providing brain sections of CB1R knock-out and control mice. The authors are grateful to Natalia Velez-Alicea (MIT, Boston, MA) for correction of the English syntax.

References

Acsady L, Gorcs TJ, Freund TF. 1996. Different populations of vasoactive intestinal polypeptide-immunoreactive interneurons are specialized to control pyramidal cells or interneurons in the hippocampus. Neuroscience. 73:317–334.

Bernard V, Laribi O, Levey AI, Bloch B. 1998. Subcellular redistribution of m2 muscarinic acetylcholine receptors in striatal interneurons in vivo after acute cholinergic stimulation. J Neurosci. 18:10207–10218.

Bodor AL, Katona I, Nyiri G, Mackie K, Ledent C, Hajos N, Freund TF. 2005. Endocannabinoid signaling in rat somatosensory cortex: laminar differences and involvement of specific interneuron types. J Neurosci. 25:6845–6856.

Childers SR. 2006. Activation of G-proteins in brain by endogenous and exogenous cannabinoids. Aaps J. 8:E112–E117.

Coutts AA, Anavi-Goffer S, Ross RA, MacEwan DJ, Mackie K, Pertwee RG, Irving AJ. 2001. Agonist-induced internalization and trafficking of cannabinoid CB1 receptors in hippocampal neurons. J Neurosci. 21:2425–2433.

Csaba Z, Bernard V, Helboe L, Bluet-Pajot MT, Bloch B, Epelbaum J, Dournaud P. 2001. In vivo internalization of the somatostatin sst2A receptor in rat brain: evidence for translocation of cell-surface receptors into the endosomal recycling pathway. Mol Cell Neurosci. 17:646–661.

D'Antona AM, Ahn KH, Kendall DA. 2006. Mutations of CB1 T210 produce active and inactive receptor forms: correlations with ligand affinity, receptor stability, and cellular localization. Biochemistry. 45:5606–5617.

Egertova M, Elphick MR. 2000. Localisation of cannabinoid receptors in the rat brain using antibodies to the intracellular C-terminal tail of CB. J Comp Neurol. 422:159–171.
Ellis J, Pediani JD, Canals M, Milasta S, Milligan G. 2006. Orexin-1 receptor-cannabinoid CB1 receptor heterodimerization results in both ligand-dependent and -independent coordinated alterations of receptor localization and function. J Biol Chem. 281: 38812–38824.
Ferguson SS. 2001. Evolving concepts in G protein-coupled receptor endocytosis: the role in receptor desensitization and signaling. Pharmacol Rev. 53:1–24.
Freund TF, Katona I, Piomelli D. 2003. Role of endogenous cannabinoids in synaptic signaling. Physiol Rev. 83:1017–1066.
Gonzalez S, Cebeira M, Fernandez-Ruiz J. 2005. Cannabinoid tolerance and dependence: a review of studies in laboratory animals. Pharmacol Biochem Behav. 81:300–318.
Hoffman AF, Oz M, Yang R, Lichtman AH, Lupica CR. 2007. Opposing actions of chronic Delta9-tetrahydrocannabinol and cannabinoid antagonists on hippocampal long-term potentiation. Learn Mem. 14:63–74.
Hoffman AF, Riegel AC, Lupica CR. 2003. Functional localization of cannabinoid receptors and endogenous cannabinoid production in distinct neuron populations of the hippocampus. Eur J Neurosci. 18:524–534.
Howlett AC, Breivogel CS, Childers SR, Deadwyler SA, Hampson RE, Porrino LJ. 2004. Cannabinoid physiology and pharmacology: 30 years of progress. Neuropharmacology. 47(Suppl 1):345–358.
Hsieh C, Brown S, Derleth C, Mackie K. 1999. Internalization and recycling of the CB1 cannabinoid receptor. J Neurochem. 73: 493–501.
Jin W, Brown S, Roche JP, Hsieh C, Celver JP, Kovoor A, Chavkin C, Mackie K. 1999. Distinct domains of the CB1 cannabinoid receptor mediate desensitization and internalization. J Neurosci. 19: 3773–3780.
Katona I, Rancz EA, Acsady L, Ledent C, Mackie K, Hajos N, Freund TF. 2001. Distribution of CB1 cannabinoid receptors in the amygdala and their role in the control of GABAergic transmission. J Neurosci. 21:9506–9518.
Katona I, Sperlagh B, Sik A, Kafalvi A, Vizi ES, Mackie K, Freund TF. 1999. Presynaptically located CB1 cannabinoid receptors regulate GABA release from axon terminals of specific hippocampal interneurons. J Neurosci. 19:4544–4558.
Katona I, Urban GM, Wallace M, Ledent C, Jung KM, Piomelli D, Mackie K, Freund TF. 2006. Molecular composition of the endocannabinoid system at glutamatergic synapses. J Neurosci. 26: 5628–5637.
Kawamura Y, Fukaya M, Maejima T, Yoshida T, Miura E, Watanabe M, Ohno-Shosaku T, Kano M. 2006. The CB1 cannabinoid receptor is the major cannabinoid receptor at excitatory presynaptic sites in the hippocampus and cerebellum. J Neurosci. 26:2991–3001.
Kobilka BK, Deupi X. 2007. Conformational complexity of G-protein-coupled receptors. Trends Pharmacol Sci. 28:397–406.
Leranth C, Frotscher M, Tombol T, Palkovits M. 1984. Ultrastructure and synaptic connections of vasoactive intestinal polypeptide-like immunoreactive non-pyramidal neurons and axon terminals in the rat hippocampus. Neuroscience. 12:531–542.
Leterrier C, Bonnard D, Carrel D, Rossier J, Lenkei Z. 2004. Constitutive endocytic cycle of the CB1 cannabinoid receptor. J Biol Chem. 279:36013–36021.
Leterrier C, Laine J, Darmon M, Boudin H, Rossier J, Lenkei Z. 2006. Constitutive activation drives compartment-selective endocytosis and axonal targeting of type 1 cannabinoid receptors. J Neurosci. 26:3141–3153.
Martin BR, Sim-Selley LJ, Selley DE. 2004. Signaling pathways involved in the development of cannabinoid tolerance. Trends Pharmacol Sci. 25:325–330.
Martini L, Waldhoer M, Pusch M, Kharazia V, Fong J, Lee JH, Freissmuth C, Whistler JL. 2006. Ligand-induced down-regulation of the cannabinoid 1 receptor is mediated by the G-protein-coupled receptor-associated sorting protein GASP1. Faseb J. 21:802–811.
Matyas F, Yanovsky Y, Mackie K, Kelsch W, Misgeld U, Freund TF. 2006. Subcellular localization of type 1 cannabinoid receptors in the rat basal ganglia. Neuroscience. 137:337–361.
Morozov YM, Freund TF. 2003. Post-natal development of type 1 cannabinoid receptor immunoreactivity in the rat hippocampus. Eur J Neurosci. 18:1213–1222.
Nyiri G, Cserep C, Szabadits E, Mackie K, Freund TF. 2005. CB(1) cannabinoid receptors are enriched in the perisynaptic annulus and on preterminal segments of hippocampal GABAergic axons. Neuroscience. 136:811–822.
Parton RG, Dotti CG. 1993. Cell biology of neuronal endocytosis. J Neurosci Res. 36:1–9.
Parton RG, Simons K, Dotti CG. 1992. Axonal and dendritic endocytic pathways in cultured neurons. J Cell Biol. 119:123–137.
Riad M, Zimmer L, Rbah L, Watkins KC, Hamon M, Descarries L. 2004. Acute treatment with the antidepressant fluoxetine internalizes 5-HT1A autoreceptors and reduces the in vivo binding of the PET radioligand [18F]MPPF in the nucleus raphe dorsalis of rat. J Neurosci. 24:5420–5426.
Rinaldi-Carmona M, Le Duigou A, Oustric D, Barth F, Bouaboula M, Carayon P, Casellas P, Le Fur G. 1998. Modulation of CB1 cannabinoid receptor functions after a long-term exposure to agonist or inverse agonist in the Chinese hamster ovary cell expression system. J Pharmacol Exp Ther. 287:1038–1047.
Siegel N, Rosner M, Unbekandt M, Fuchs C, Slabina N, Dolznig H, Davies JA, Lubec G, Hengstschlager M. 2010. Contribution of human amniotic fluid stem cells to renal tissue formation depends on mTOR. Hum Mol Genet. 19:3320–3331.
Sim LJ, Selley DE, Dworkin SI, Childers SR. 1996. Effects of chronic morphine administration on mu opioid receptor-stimulated [35S] GTPgammaS autoradiography in rat brain. J Neurosci. 16: 2684–2692.
Sim-Selley LJ. 2003. Regulation of cannabinoid CB1 receptors in the central nervous system by chronic cannabinoids. Crit Rev Neurobiol. 15:91–119.
Sim-Selley LJ, Martin BR. 2002. Effect of chronic administration of R-(+)-[2,3-Dihydro-5-methyl-3-[(morpholinyl)methyl]pyrrolo [1,2,3-de]-1,4-b enzoxazinyl]-(1-naphthalenyl)methanone mesylate (WIN55,212-2) or delta(9)-tetrahydrocannabinol on cannabinoid receptor adaptation in mice. J Pharmacol Exp Ther. 303:36–44.
Sim-Selley LJ, Vogt LJ, Xiao R, Childers SR, Selley DE. 2000. Region-specific changes in 5-HT(1A) receptor-activated G-proteins in rat brain following chronic buspirone. Eur J Pharmacol. 389:147–153.
Sinclair GI, Baas PW, Heidemann SR. 1988. Role of microtubules in the cytoplasmic compartmentation of neurons. II. Endocytosis in the growth cone and neurite shaft. Brain Res. 450:60–68.
Tsao P, Cao T, von Zastrow M. 2001. Role of endocytosis in mediating downregulation of G-protein-coupled receptors. Trends Pharmacol Sci. 22:91–96.
Tsou K, Mackie K, Sanudo-Pena MC, Walker JM. 1999. Cannabinoid CB1 receptors are localized primarily on cholecystokinin-containing GABAergic interneurons in the rat hippocampal formation. Neuroscience. 93:969–975.
Turu G, Simon A, Gyombolai P, Szidonya L, Bagdy G, Lenkei Z, Hunyady L. 2007. The role of diacylglycerol lipase in constitutive and angiotensin AT1 receptor-stimulated cannabinoid CB1 receptor activity. J Biol Chem. 282:7753–7757.
Uchigashima M, Narushima M, Fukaya M, Katona I, Kano M, Watanabe M. 2007. Subcellular arrangement of molecules for 2-arachidonoyl-glycerol-mediated retrograde signaling and its physiological contribution to synaptic modulation in the striatum. J Neurosci. 27:3663–3676.
Wu DF, Yang LQ, Goschke A, Stumm R, Brandenburg LO, Liang YJ, Hollt V, Koch T. 2008. Role of receptor internalization in the agonist-induced desensitization of cannabinoid type 1 receptors. J Neurochem. 104:1132–1143.
Yoshida T, Fukaya M, Uchigashima M, Miura E, Kamiya H, Kano M, Watanabe M. 2006. Localization of diacylglycerol lipase-alpha around postsynaptic spine suggests close proximity between production site of an endocannabinoid, 2-arachidonoyl-glycerol, and presynaptic cannabinoid CB1 receptor. J Neurosci. 26:4740–4751.